A Study on the Behavior and Heat Transfer Characteristics of Impinging Sprays

Hei Cheon, Yang*†, Sang Kyoo, Park

Division of Mechanical and Automotive Engineering, Yosu National University

The spray/wall interaction is considered as an important phenomenon influencing air-fuel mixing in the internal combustion engines. In order to adequately represent the spray/wall interaction process, impingement regimes and post-impingement behavior have been modeled using experimental data and conservation constraints. The modeled regimes were stick, rebound, spread and splash. The tangential velocities of splashing droplets were obtained using a theoretical relationship. The continuous phase was modeled using the Eulerian conservation equations, and the dispersed phase was calculated using a discrete droplet model. The numerical simulations were compared to experimental results for spray impingement normal to the wall. The predictions for the secondary droplet velocities and droplet sizes were in good agreement with the experimental data.

Key Words : Impinging Spray, Spray/Wall Interaction, Impingement Regime, Post-Impingement Behavior, Splashing Droplet

Nomenclature

D : Droplet diameter
f : Frequency of the impinging droplet
h : Height of splashing lamella
K : Non-dimensional parameter $(=Oh \cdot \mathrm{Re}_{bn}^{1.25})$
m : Droplet mass
N : Number of droplets in a parcel
Oh : Ohnesorge number $(=\rho_d D_b v_{bn}/\mu_d)$
Re : Reynolds number $(=\mu_d/\rho_d \sigma_d D_b)$
r_c : Radius of splashing lamella
r_m : Splashing mass ratio
v : Velocity of droplet
We_c : Critical Weber number based on the incident droplet velocity
θ_b : Incident angle of impinging droplets measured from the wall
θ_b : Splashing angle of droplets measured from the wall
σ : Surface tension of the droplet
φ : Time fraction at which the splash occurs
ν : Kinematic viscosity of the impinging droplet

Subscripts

a, b : After and before impingement, respectively
n, t : Normal and tangential, respectively
d, s : Droplet and splashing, respectively

† First Author
* Corresponding Author,
E-mail : hcyang@yosu.ac.kr
TEL : +82-61-640-6222 ; FAX : +82-61-640-6228
Division of Mechanical and Automotive Engineering, Yosu National University 195 Kuk Dong, Yosu, Chonnam, 550-749, Korea. (Manuscript **Received** June 21, 2000; **Revised** December 15, 2000)

1. Introduction

The characteristics of droplet impingement on a surface are of importance in many applications. Especially, fuel spray/wall interaction is considered as an important phenomenon influencing air-fuel mixing in the internal combustion engines. The interaction processes are fully coupled and strongly influence engine performance and emissions in both compression ignition and spark ignition engines. Therefore, it is very significant to understand the characteristics of spray/wall interaction to design more effective engines and to reduce air pollution.

Detailed information about the droplet dynamics in the vicinity of a wall is required to characterize spray/wall interaction and its effect on secondary breakup and fuel/air mixing as well as the structure of developing wall-jet. However it is extremely difficult to obtain detailed information of impinging spray through experiment in engines. Recently Arcoumanis and Chang(1993, 1994) investigated a transient behavior of the two-phase wall-jet and the effect of wall temperature on the wall-jet dynamics using a phase Doppler anemometer to obtain simultaneous measurements of spray droplet sizes and velocities in the proximity of the wall. Also an investigation of the transient DI diesel spray impinging on a flat wall was performed using a phase Doppler velocimeter by Schunemann et al. (1998).

Computational modeling, however, offers a promising alternative for the purpose of obtaining detailed information on impinging spray characteristics. The first attempt was that of Naber and Reitz(1988), who developed a model to study spray impingement using the KIVA code. As an improvement in spray-wall interaction process, a wall heat transfer model was developed by Eckhause and Reitz(1995).

Watkins and Wang(1990) proposed a model which differed with that of Naber and Reitz (1988). Their model was initially found to significantly underpredict wall spray dispersion compared to experimental data. Park(1994), Park and Watkins(1996) developed a different impingement model. It was based on Wachters and Westerling's data(1966) of spreading of the liquid film about the central dome as a droplet deformed after impact on a hot solid or liquid surface.

In the model of Senda et al. (1994), correlations were proposed for impingement on unheated or heated surface. The fuel film formation and its breakup due to the impinging droplets were taken into account. Nagaoka et al. (1994) published a paper for spray impingement on hot surfaces applied to the port injection gasoline engines. Senda et al. (1996) considered the superheating degree of a surface for the liquid saturation temperature and proposed a new spray

impingement model considering droplet-droplet interaction near the wall and fuel film formation process on the wall.

Bai and Gosman(1995) proposed a spray impingement model which was formulated on the basis of literature findings and mass, momentum and energy conservation constraints. The model involved an analysis of the relevant impingement regimes and the associated post-impingement characteristics. Bai and Gosman(1996), Ahmadi-Befrui et al. (1996) proposed a mathematical model of formation and transport of liquid films incorporating a droplet-wall impingement model and exchange mechanisms with the gas-phase.

Stanton and Rutland(1996, 1998) developed the models considering wall film formation, its dynamics, multi-component vaporization and the modified wall functions. The major physical effects considered in the models included mass and momentum contributions to the film due to spray impingement, splashing effects, various shear forces, piston acceleration, and dynamic pressure effects. In order to adequately represent the droplet interaction process, impingement regimes and post-impingement behavior was modeled using the experimental data and mass, momentum and energy conservation constraints. Their models were based on the experimental works by Yarin and Weiss(1995) and Mundo et al. (1995a).

Mundo et al. (1995b, 1998) proposed and validated a new droplet-wall impingement model based on detailed experimental investigations to calculate near-wall polydispersed spray flows. The model was based on the definition of the value K, which incorporated both the kinematic parameters of the impinging droplet relative to the wall and the fluid properties.

Since the previous results about the effects of spray impingement in IC engines were inconsistent, it was more apparent how complicated the processes of injection, atomization, impingement and combustion were in the engine. Therefore, to better understand how the variables in these individual processes influenced the overall engine performance and emissions, it was often necessary to concentrate on a single process occurring in the

engine. The goal of this research was to investigate the characteristics of impinging spray and their post-impingement processes as related to IC engines. So, we described a different model for the simulation of spray/wall interaction within the framework of the Lagrangian approach. The model was formulated on the basis of literature findings on the processes of splashing droplets and the conservation constraints. In the next section the theoretical model was described followed by discussion of the results and conclusions.

2. Theoretical Model

2.1 Governing equations and numerical method

The continuous phase (surrounding gas) was modeled using the Eulerian conservation equations of mass, momentum, energy and turbulent transport was modeled using the modified k-ε turbulence model proposed by Reynolds (1980). The dispersed phase (droplet parcel) equations of trajectory, momentum, mass and energy were in a Lagrangian form. Each droplet parcel contained a large number of identical and non-interacting droplets. Following the start of injection, various spray sub-models; the liquid core atomization model of Reitz (1987), the secondary break-up model of Reitz and Diwaker (1987), the droplet collision and coalescence model of O'Rouke (1981) and the droplet evaporation model of Borman and Johnson (1962), were used to simulate the behavior of free spray. The effects of dispersed phase on the continuous phase were given as sources or sinks in the continuous phase equations. Thus, two phases were fully coupled, including evaporation of liquid fuel. The approach used here for the solution of these equations was resembled with the one developed by Watkins (1989). The discretisation was based on the finite volume method. The spatial discretisation scheme was a hybrid upwind/central difference scheme and the Euler implicit method was used for transient term. The discretised equations were solved subject to the appropriate initial and boundary conditions using a time-marching implicit numerical method.

2.2 Spray/wall impingement model

In general, the impingement regimes are determined by the parameters describing the pre-impingement droplets, the wall surface conditions and the surrounding gas characteristics in a near-wall region. Of particular interest in identifying impingement regimes is the wall temperature as stated by Bai and Gosman (1995). In this study, the regimes modelled for spray/wall interaction are stick, rebound, spread and splash for the wall temperature below the liquid boiling temperature.

The stick regime occurs when the impingement energy is extremely low, and the wall temperature is below the pure adhesion temperature. A droplet in this regime is assumed to coalesce completely with local film. The transition criterion for this regime is $We_c \leq 5$. The rebound regime occurs when the impingement energy is low. In this regime, the rebound droplet velocity magnitude and direction need to be determined. In this study, Bai and Gosman's method (1995) is used. The transition criterion for this regime is $5 < We_c \leq 10$. The criteria of the stick and rebound regimes are based on the experimental results of Rodrigues and Mesler (1985). The critical Weber number We_c is calculated using the normal velocity of incident droplet. The spreading regime is similar to the stick regime but occurs at higher We_c. In this regime, the droplet merges with the liquid film after impingement. The transition criterion for spreading is $10 < We_c \leq 18^2 D_b \left[\frac{\rho_d}{\sigma_d} \right]^{1/2} \nu^{1/4} f^{3/4}$. The criterion is based on the experimental results of Yarin and Weiss (1995).

The final regime is splashing and occurs at high impingement energy. The transition criterion for spreading is $We_c > 18^2 D_b \left[\frac{\rho_d}{\sigma_d} \right]^{1/2} \nu^{1/4} f^{3/4}$. New splash regime is proposed using the theoretical and experimental data of Yarin and Weiss (1995) and Mundo et al. (1995). In this regime, many quantities need to be calculated in order to describe the splashing process. These quantities include the proportion of incident droplet mass deposited as part of the liquid film and the sizes, velocities and splashing angles of secondary droplets and those are based on their experimental

results.

The tangential velocity of splashing droplet v_{at} is determined using the theoretical equation of the crown radius of splashing lamella of Yarin and Weiss(1995). Equations (1) and (2) present the height and the radius of splashing lamella.

$$h \approx (\nu/f)^{1/2} = \frac{D_b}{\text{Re}_{bn}^{1/2}} \tag{1}$$

$$\frac{r_c}{D_b} = \left(\frac{2}{3}\right)^{1/4} \cdot \frac{v_{bn}^{1/2}}{D_b^{1/4} h^{1/4}} \cdot (t - t_0)^{1/2} \tag{2}$$

Differentiating Eq. (2) and considering the time that the splash occurs and the splashing dome disappears, the velocity v_{at} yields

$$v_{at} = 0.452 \cdot \text{Re}_{bn}^{1/8} \cdot \frac{v_{bn}}{\sqrt{\psi}} \tag{3}$$

This procedure is similar to Lee's one(1998, 2000).

Using Mundo et al.'s(1995) droplet size distribution after impingement, the splashing droplet diameter D_a can be given as follows.

$$\frac{D_a}{D_b} = 3.932 \times 10^2 \times K^{-1.416} \tag{4}$$

Where K is a non-dimensional parameter. For the splashing droplet number N_a, the following equation is obtained.

$$N_a = r_m \frac{D_b^3}{D_a^3} \tag{5}$$

Where the splashing mass ratio r_m is given using Yarin and Weiss's result(1995).

$$r_m = \frac{m_s}{m_d} = -27.2 + 3.15u - 0.116u^2 + 1.4 \times 10^{-3} u^3 \tag{6}$$

Concerning the splashing angle θ_a, Mundo et al. (1995) investigated the correlation with impingement angle θ_b. The angle θ_a is given by

$$\theta_a = 61.293 + 0.3544 \theta_b \tag{7}$$

Once the tangential component of velocity and the splashing angle are known, the normal component of velocity can be calculated by

$$v_{an} = v_{at} \tan \theta_a \tag{8}$$

The wall film model is similar to the model of Nagaoka et al. (1994) that the radius and height of film are determined using the curve-fitted data of Xiong and Yuen(1991).

3. Results and Discussions

Arcoumanis and Chang's experimental results (1993, 1994) provided an evidence concerning the effects that the presence of the flat wall exerts on the droplet size and tangential velocity of the spray. The simulation conditions used in this work are shown in Table 1 which are their experimental conditions.

To begin with, to validate the free spray characteristics before impingement, a free spray simulation is performed. For the free spray condition, as shown in Fig. 1 (a), the grid consists of $40 \times 40 \times 60$ numerical nodes and occupying a volume of $50 \times 50 \times 180$ mm^3 in the x, y, z direction, respectively. The temporal histories of the droplet velocity and SMD at the nozzle exit shown in Fig. 2 are deduced from the measurements of Arcoumanis and Chang(1993) at 10mm below nozzle exit and the nozzle exit boundary conditions are used in this simulations. Although, in present computer code the wave breakup model can be used for the calculation of liquid fuel core atomization, the

Table 1 Specification of calculation conditions

Wall distance (mm)	free spray and 30
Wall temperature (K)	293 and 423
Gas temperature (K)	293
Gas pressure (bar)	1
Nozzle diameter (mm)	0.22
Injection angle (°)	90
Injection duration (ms)	1.0
Fuel injected (mm^3/pulse)	4.0
Fuel density (g/cm^3)	0.825
Ambient gas	Air
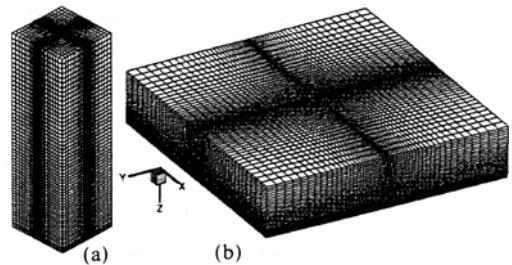
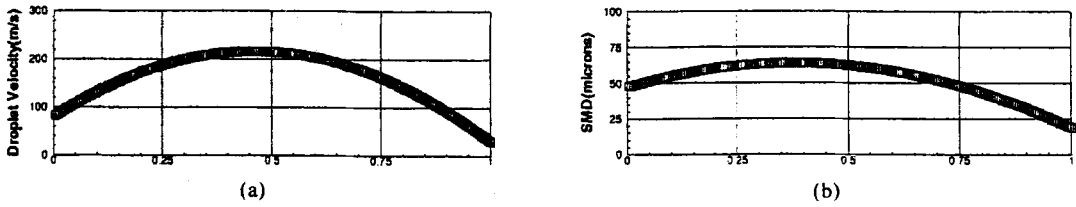**Fig. 1** Numerical grid (a) for free spray calculation (b) for impinging spray calculation

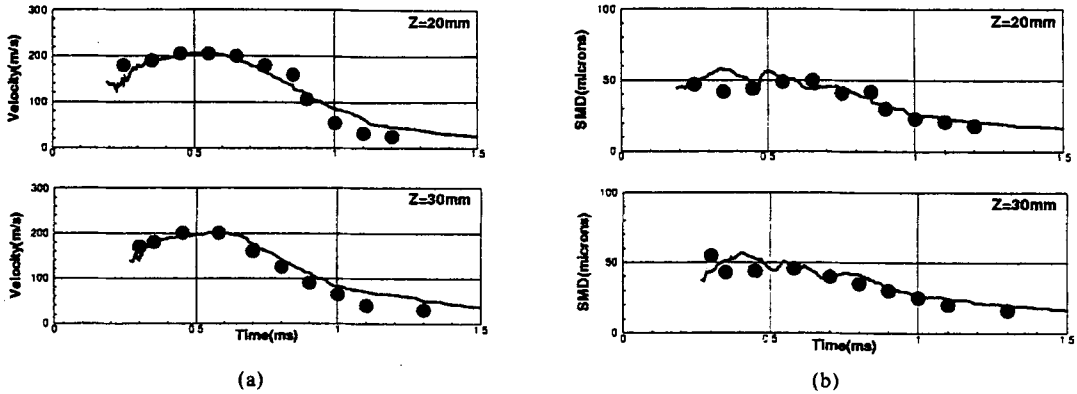Fig. 2 Nozzle exit boundary conditions (a) droplet injection velocity (b) droplet SMD

Fig. 3 Comparison between the computational and the experimental results at 20 and 30 mm from the nozzle
(a) for centerline droplet axial velocity (b) for centerline droplet SMD

deduced data are used because more accurate free spray characteristics before impingement are required to validate a new spray/wall interaction model as stated by Gavaises(1997).

Figures 3(a) and (b) show the comparisons between the computational and experimental results for the centerline droplet axial mean velocity and SMD at 20 and 30mm below the injection nozzle. In general, the trend of calculations is in qualitatively good agreement with the measurements. The droplet sizes decrease with distance from the injection nozzle and that is attributed to secondary droplet breakup effects. Afterwards the time of the maximum velocity, smaller droplets seem to pass through the control volume, and at the latest stages of injection smaller droplet sizes are predicted in agreement with the experimental data. It should be noted, however, that these droplets have been formed earlier during the injection period. The smaller droplets decelerate very quickly compared to the larger ones and pass through the control volume after a considerable time. Thus, the temporal profile of the SMD does not actually relate smaller droplets to smaller

injection velocities.

For the impinging spray simulation, as shown in Fig. 1(b), the grid of $60 \times 60 \times 40$ numerical nodes are non-uniformly distributed and a volume of $180 \times 180 \times 35$ mm³ in the x, y, z direction are occupied. The grid resolution was found to give adequately grid-independent results performed by Lee and Ryou(2000). The injection direction coincides with the z-direction. Comparisons are preformed along the wall at radial distances of 6, 10 and 15mm from the free spray axis and at three locations from the wall of 0.5, 3.0 and 5.0 mm as shown in Fig. 4. These measuring locations correspond to representative regions of the two-phase wall-jet; the main wall-jet region, the stagnation region and the downstream region, as stated by Arcoumanis and Chang(1994). In this simulation, a total of 6000 droplet parcels are used. The numerical results using the Lee's model and the proposed model are compared with the experimental results of Arcoumanis and Chang (1994).

Figures 5(a) and (b) show the development of the induced velocity field and the spray impinging
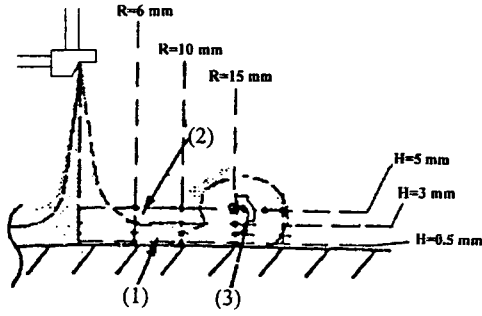
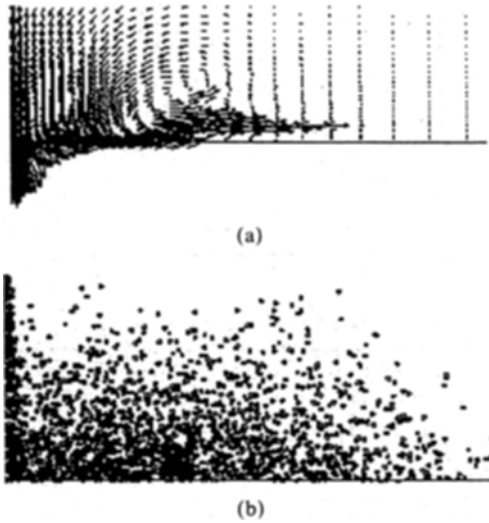**Fig. 4** Measurement positions within the two-phase wall-jet flow

(a)

(b)

Fig. 5 Development of impinging (a) gas velocities (b) spray droplets at 1.2 ms after the start of injection

Fig. 6 Droplet mean tangential velocity at 0.5 mm from the impinging wall
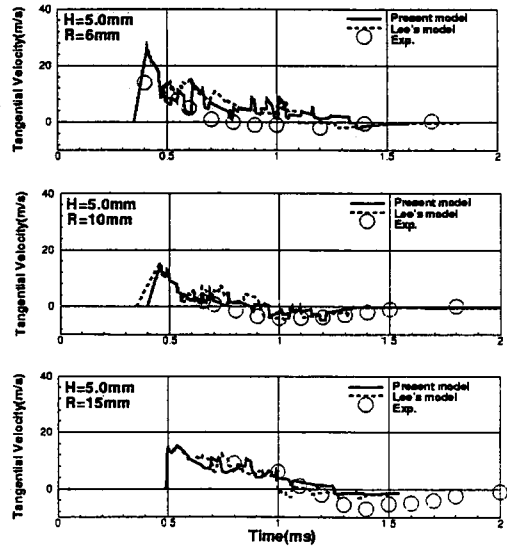
Fig. 7 Droplet mean tangential velocity at 5.0 mm from the impinging wall

on the flat wall at 1.2ms after the start of injection for a wall temperature of 150 ℃. The induced velocity profiles reveal a wall-jet emanating radially outward from the impinging region, near the tip of which there is an irregular-shape main vortex. It is this vortex which influences the movement of droplets, especially the smaller secondary droplets that result from splashing. Also as can be seen, a smaller vortex occurs near the wall as the main vortex is progressively stretched at later times.

The temporal behaviour of the tangential velocities is compared in Figs. 6 and 7. Figure 6 contains the results obtained at a height of 0.5 mm from the wall and radial distances of 6, 10 and 15 mm for T=20 ℃. For the tangential velocity
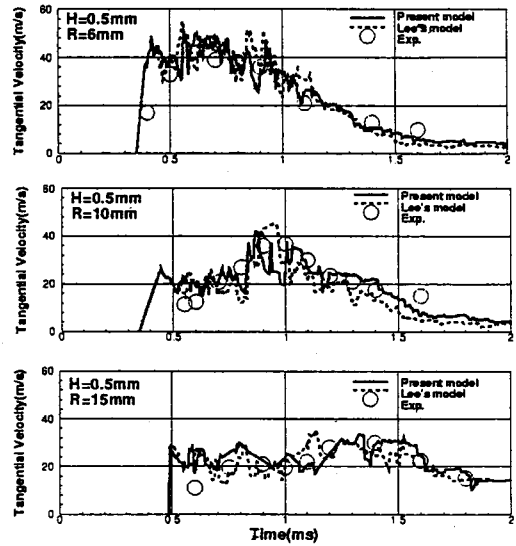
profiles near the wall, the predicted results show similar trends as the experimental data. As the radial distance increases, the maximum tangential velocity decreases as the liquid wall-jet is decelerated. Figure 7 is the results obtained at a height of 5.0 mm from the wall and radial distances of 6, 10 and 15 mm, respectively, for T=20 ℃. As can be seen, at 6 mm radial distance, the tangential velocity starts at a maximum velocity and then

decays to nearly zero, while at radial distances of 10 and 15 mm, the tangential velocity starts at a maximum velocity and then decays to below zero before increasing again. The peak values of the tangential velocity of the droplets become smaller due to the loss of momentum of the droplets with increasing radial distance. By comparing the tangential velocities at different heights, it becomes apparent that most of droplet tangential velocity

remains concentrated in the region near the wall surface during the main injection period.

The temporal behaviour of the droplet SMD is compared in Figs. 8 and 9. The trends of SMD are similar to that of measurements. As the distance from the wall surface increases, the droplet size decreases. This provides further evidence that the majority of the droplet momentum remains concentrated in the region near the wall surface. It is interesting to note that the tangential velocity and the droplet diameter curves show fluctuation. The reason may be attributed to the fact that the spray tip velocity is fluctuated because the droplets of the tip meet the highest aerodynamic resistance and then slow down, therefore the droplets retarded at the tip are continually replaced by later-injected, higher-momentum droplets.

Figures 10 and 11 show the results on the effect of wall temperature on the tangential velocity and the droplets size. No clear trends are evident between the high temperature and low tempera-
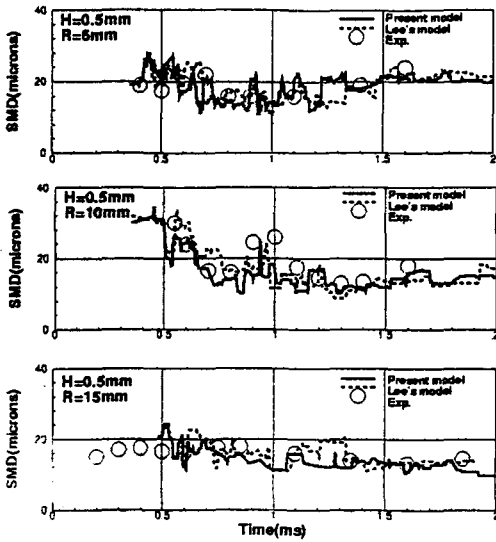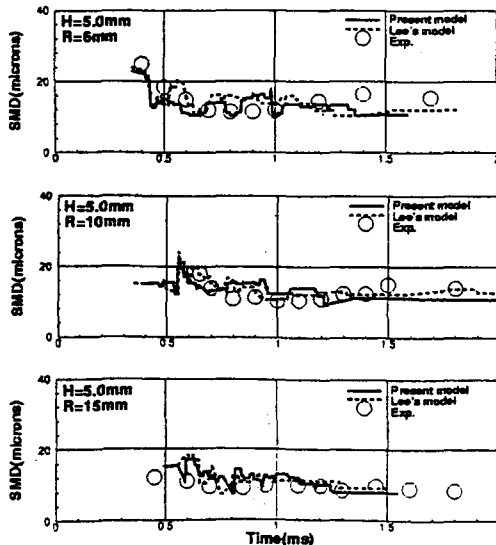

Fig. 8 Droplet SMD at -0.5 mm from the impinging wall

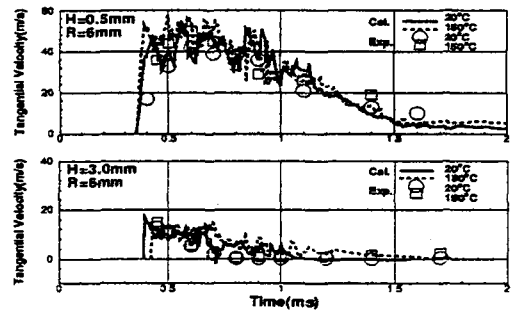**Fig. 9** Droplet SMD at 5.0 mm from the impinging wall

Fig. 10 Effect of wall temperature on droplet tangential velocity at radial distance 6 mm
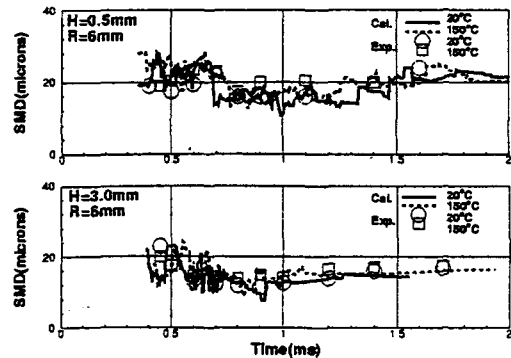

Fig. 11 Effect of wall temperature on droplet size at radial distance 6 mm
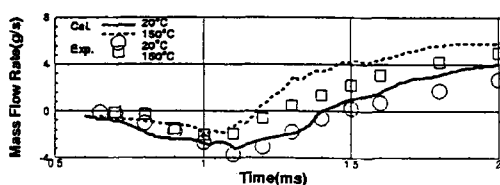
Fig. 12 Effect of wall temperature on air entrainment ratio into wall-jet

ture cases. However in most cases, the simulated results provide similar trends. The tangential velocities are greater than in the high wall temperature case. This may be attributed to the interaction of turbulent air flow resulting from enhanced air entrainment as the wall vortex moves radially with higher velocity. The effect of wall temperature on the tangential velocity becomes less noticeable farther from the wall.

Figure 12 presents the effect of wall temperature on air entrainment. Arcoumanis and Chang (1994) calculated the mass flowrate of air entrained into the wall-jet based on the normal velocity component of the droplets at a height of 5.0 mm from the surface and measured between radial distances of 10 and 20 mm over a 50 μs time interval. By assuming symmetry about the spray axis, they evaluated the entrained mass flowrate using the expression:

$$m_e = \int_{R=10}^{R=20} \rho_a 2\pi R v_{an} dR \qquad (9)$$

Where v_{an} is the splashing droplet normal velocity, ρ_a the air density and R the radial distance from the spray axis. In this study, the mass flowrate is calculated in a similar manner as the Eq. (9) except that the air normal velocity is used instead of the droplet normal velocity. The result reveals that initially the mass flowrate is negative due to the passage of the wall-jet head that pushes the air away from the wall, and then positive entrainment of the air starts and increases at the latter stage of impingement. The entrainment of air increases with wall temperature and the air entrainment into the wall-jet occurs earlier for the high temperature case. This tends to suggest that the higher wall temperature is more effective in inducing air entrainment into the wall

-jet and enhancing fuel-air mixing in impinging diesel sprays.

4. Conclusions

To investigate the characteristics of the impinging droplets and their post-impingement processes as related to IC engines, a spray/wall interaction model has been formulated within the framework of the Lagrangian approach. The model is formulated on the basis of literature findings on the processes of splashing and the conservation constraints for the droplets. The model is validated through a series of comparisons to the wall spray experimental data and the numerical results using a Lee's model. The model provided relatively good agreement for free and impinging spray characteristics. As for secondary droplet characteristics, the models capture the correct trends for droplet velocities and sizes over the majority of the injection period. However more validation works are necessary and the transient behavior of the film model should be considered by solving the film equations to enhance the predictive capabilities of the present model.

Acknowledgment

References

Ahmadi-Befrui, B., Uchil, N, Gosman, A. D. and Issa, R. I., 1996, "Modelling and Simulation of Thin Liquid Films Formed by Spray-Wall Interaction," SAE 960627.

Arcoumanis, C. and Chang, J-C., 1993, "Heat Transfer Between a Heated Plate and an Impinging Transient Diesel Spray," *Experiments in Fluids*, Vol. 16, pp. 105~119.

Arcoumanis, C. and Chang, J-C., 1994, "Flow and Heat Transfer Characteristics of Impinging Transient Diesel Spray," SAE 940678.

Bai, C. and Gosman, A. D., 1995, "Development of Methodology for Spray Impingement

Simulation," SAE 950283.

Bai, C. and Gosman, A. D., 1996, "Mathematical Modelling of Wall Films Formed by Impinging Spray," SAE 960626.

Borman, G. L. and Johnson, J. H., 1962, "Unsteady Vaporisation Histories and Trajectories of Fuel Drops Injected into Swirling Air," SAE 598C.

Eckhause, J. E. and Reitz, R. D., 1955, "Modelling Heat Transfer to Impinging Fuel Sprays in Direct-Injection Engines," *Atomization and Sprays*, Vol. 5, pp. 213~242.

Gavaises, M., 1997, "Modelling of Diesel Fuel Injection Processes," PhD thesis, Imperial College of Science, Technology and Medicine, University of London.

Lee, S. H., 1998, "Development of a New Model and Heat Transfer Analysis of Impinging Diesel Sprays on a Wall," PhD thesis, Chung-Ang University.

Lee, S. H., Ryou, H. S., 2000, "Modelling of Diesel Spray Impingement on a Flat Wall," *KSME International Journal*, Vol. 21, No. 2, pp. 151~173.

Mundo, C., Sommerfeld, M. and Tropea, C., 1995a, "Droplet-Wall Collisions: Experimental Studies of the Deformation and Breakup Process," *Int. J. Multiphase Flow*, Vol. 21, No. 2, pp. 151~173.

Mundo, C., Sommerfeld, M. and Tropea, C., 1995b, "Numerical and Experimental Investigation of Spray Characteristics in the Vicinity of a Right Wall," *ICLASS 95, Two Phase Flow Modelling And Experiment*, Rome.

Mundo, C., Sommerfeld, M. and Tropea, C., 1998, "On the Modelling of Liquid Sprays Impinging on Surfaces," *Atomization and Sprays*, Vol. 8, pp. 625~652.

Naber, J. D. and Reitz, R. D., 1988, "Modelling Engine Spray/Wall Impingement," SAE 880107.

Nagaoka, M., Kawazoe, H. and Nomura, N., 1994, "Modelling Fuel Spray Impingement on a Hot Wall for Gasoline Engines," *SAE 940525*.

O'Rourke, P. J., 1981, "Collective Drop Effects on Vaporizing Liquid Sprays," PhD thesis, Princeton University, Princeton, NJ.

Park, K., 1994, "Development of a Non-Orthogonal-Grid Computer Code for the Optimization of Direct-Injection Diesel Engine Combustion Chamber Shapes," PhD thesis, University of Manchester Institute of Science and Technology.

Park, K. and Watkins, A. P., 1996, "Comparison of Wall Spray Impaction Models with Experimental Data on Drop Velocities and Sizes," *Int. Heat and Fluid Flow*, Vol. 17, No. 4, pp. 424 ~438.

Reitz, R. D., 1987, "Modelling Atomization Processes in High-pressure Vaporizing Sprays," *Atomization and Spray Tech*, Vol. 3, pp. 309 ~337.

Reitz, R. D. and Diwakar, D., 1987, "Structure of High Pressure Fuel Sprays," SAE 870598.

Reynolds, W. C., 1980, *Modelling of Fluid Motions in Engines-an Introductory Overview, in Combustion Modelling in Reciprocating Engines*, ed. J. N. Mattavi and C. A. Amann, Plenum Press, NY.

Rodrigues, F. and Mesler, R., 1985, "Some Drops Don't Splash," *J. of Colloid and Interface Science*, Vol. 106, No. 2, pp. 347~352.

Schunemann, E., Fedrow, S. and Leipertz, A., 1998, "Droplet Size and Velocity Measurements for the Characterization of a DI Diesel Spray Impinging on a Flat Wall," SAE 982545.

Senda, J., Kobayashi, M., Iwashita, S. and Fujimoto, H., 1994, "Modelling of Diesel Spray Impingement on a Flat Wall," SAE 941894.

Senda, J., Kanda, T., Al-Roub, M., Farrell, P. V., Fukami, T. and Fujimoto, H., 1997, "Modelling Spray Impingement Considering Fuel Film Formation on the Wall," SAE 970047.

Stanton, D. W. and Rutland, C. J., 1996, "Modelling Fuel Film Formation and Wall Interaction in Diesel Engines," SAE 960628.

Stanton, D. W. and Rutland, C. J., 1998, "Multi-dimensional Modelling of Thin Liquid Films and Spray Wall Interactions Resulting from Impinging Sprays," *Int. J. Heat and Mass Transfer*, Vol. 41, pp. 3037~3054.

Watchters, L. H. J. and Westerling, N. A. J., 1966, "The Heat Transfer from a Hot Wall to Impinging Water Drops in a Spheroidal State," *Chem. Eng. Sic.*, Vol. 21, pp. 1047~1056.

Watkins, A. P., 1989, "Three-dimensional

Modelling of Gas Flow and Sprays in Diesel Engines," *In Computer Simulation of Fluid Flow, Heat and Mass Transfer and Combustion in Reciprocating Engines*, N. C. Markatos (ed), Hemisphere, Bristol, PA, pp. 193~237.

Watkins, A. P, and Wang, D. M., 1990, "A New Model for Diesel Spray Impaction on Walls and Comparison with Experiment," *Int. Symp. on Diagnostics and Modelling of Combustion in IC Engines*, Kyoto, pp. 243~248.

Xiong, T. Y. and Yuen, M. C., 1991, "Evaporation of a Liquid Droplet on a Hot Plate," *Int. J. Heat and Mass Transfer*, Vol. 34, No. 7, pp. 1881~1894.

Yarin, A. L. and Weiss, D. A., 1995, "Impact of Drops on Solid Surfaces: Self-similar Capillary Waves and Splashing as a New Type of Kinematic Discontinuity," *J. Fluid Mech.*, Vol. 283, pp. 141~173.